applied sciences

MDPI

Review

Recent Advances in Equalization Technologies for Short-Reach Optical Links Based on PAM4 Modulation: A Review

Honghang Zhou, Yan Li *, Yuyang Liu, Lei Yue, Chao Gao, Wei Li, Jifang Qiu, Hongxiang Guo, Xiaobin Hong, Yong Zuo and Jian Wu *

The State Key Laboratory of Information Photonics and Optical Communications, Beijing University of Posts and Telecommunications, Beijing 100876, China; zhh1994@bupt.edu.cn (H.Z.); yuyangliu@bupt.edu.cn (Y.L.); leiyuebupt@outlook.com (L.Y.); gcg@bupt.edu.cn (C.G.); w_li@bupt.edu.cn (W.L.); jifangqiu@bupt.edu.cn (J.Q.); hxguo@bupt.edu.cn (H.G.); xbhong@bupt.edu.cn (X.H.); yong_zuo@bupt.edu.cn (Y.Z.)

* Correspondence: liyan1980@bupt.edu.cn (Y.L.); jianwu@bupt.edu.cn (J.W.)

Received: 2 May 2019; Accepted: 3 June 2019; Published: 7 June 2019

Abstract: In recent years, short-reach optical links have attracted much more attention and have come to constitute a key market segment due to the rapid development of data-center applications and cloud services. Four-level pulse amplitude modulation (PAM4) is a promising modulation format to provide both a high data rate and relatively low cost for short-reach optical links. However, the direct detector and low-cost components also pose immense challenges, which are unforeseen in coherent transmission. To compensate for the impairments and to truly meet data rate requirements in a cost-effective manner, various digital signal processing (DSP) technologies have been proposed and investigated for short-reach PAM4 optical links. In this paper, an overview of the latest progress on DSP equalization technologies is provided for short-reach optical links based on PAM4 modulation. We not only introduce the configuration and challenges of the transmission system, but also cover the principles and performance of different equalizers and some improved methods. Moreover, machine learning algorithms are discussed as well to mitigate the nonlinear distortion for next-generation short-reach PAM4 links. Finally, a summary of various equalization technologies is illustrated and our perspective for the future trend is given.

Keywords: short-reach optical links; direct detection; four-level pulse amplitude modulation; digital signal processing; equalization

1. Introduction

Driven by upcoming services such as the Internet of Things (IoT), 4K/8K video applications, virtual reality (VR) and big data, the global internet protocol (IP) traffic has grown explosively in recent years [1]. As predicted by a Cisco report [2], 4.8 zettabytes of annual global IP traffic will be reached by 2022 and the so-called "Zettabyte Era" has arrived. To accommodate the associated demands, short-reach optical links have been widely investigated for data center interconnects (DCI), metro network, optical access, and so forth [3]. Unlike long-reach transmission, the short-reach optical links are especially sensitive to cost and size due to the large scale of their deployment [4]. Therefore, intensity modulation with direct detection (IM/DD) is adopted as the mainstream solution instead of coherent detection [5–7]. Traditional IM/DD optical interconnects implemented with non-return-to-zero on-off-keying (NRZ-OOK) format struggle to support the requirements of the increased transmission rate. Thus, many advanced modulation formats are employed to improve the spectrum efficiency (SE) and reduce the bandwidth limitation for electronic and optical components [8–17], such as four-level pulse amplitude modulation (PAM4), carrier-less amplitude and phase modulation (CAP), discrete

multi-tone (DMT), and quadrature amplitude modulation (QAM) based on Kramers-Kronig (KK) receiver [18]. Considering the power consumption and implementation complexity, the most attractive format in short-reach optical links is PAM4, which is believed as a highly promising candidate for the next-generation passive optical network (NG-PON) and has been ratified by IEEE 802.3 bs for 400 Gbps Ethernet transmission [19–25].

However, the low-pass filtering effects induced by the limited bandwidth of transmitter and receiver can cause severely inter-symbol interference (ISI). Low-cost devices such as lasers, modulators, photodiodes (PD) and trans-impedance amplifiers (TIA) also produce nonlinear distortions like level-dependent skew and level-dependent noise. Furthermore, the interaction between chromatic dispersion (CD) and direct detection will lead to a power-fading effect, where the detected signal may contain frequency notches after several kilometers transmission at a high symbol rate. Therefore, various equalization technologies based on digital signal processing (DSP) have been investigated for short-reach links over the years [26–53]. Conventional equalizers, such as the feed-forward equalizer (FFE) or decision feedback equalizer (DFE), are employed to compensate for the linear impairments induced by limited bandwidth and CD [26–28], while the equalizer based on the Volterra series is utilized to mitigate nonlinear distortion [29–32]. Some new equalization techniques, such as direct detection-faster than Nyquist (DD-FTN) algorithm [33–35], intensity directed FFE/DFE (ID-FFE/ID-DFE) algorithm [36,37] and joint clock recovery and FFE (CR-FFE) algorithm [38,39], have recently been proposed to solve different problems in practical implementation. In addition, machine learning methods like support vector machine (SVM) [40–42] and neural network (NN) [43–53] have been investigated to further eliminate system impairments for PAM4 modulation.

In this paper, an overview is provided on the important topic of advanced DSP for short-reach PAM4 optical links. The rest of this paper is organized as follows. In Section 2, the system configuration is introduced for short-reach PAM4 transmission in detail, where the comparisons for different transmitters and receivers are presented as well. Section 3 describes the distortions of high-speed transmission with low cost, including limited bandwidth, CD, nonlinear devices and power fading effect. To deal with these impairments in practical implementation, the principles of conventional FFE/DFE and improved algorithms based on FFE/DFE are first illustrated in Section 4. Moreover, VNLE and equalization based on machine learning are also discussed here. Furthermore, a summary of various equalization technologies is given in Section 4. Finally, conclusions are drawn in Section 5.

2. System Configuration

The typical system configuration for short-reach optical links based on PAM4 modulation is presented in Figure 1. The origin data generated by pseudorandom binary sequence (PRBS) is first encoded by a forward error correction (FEC) encoder and then mapped to the PAM4 symbol. After resampling and pulse shaping, the digital signal is pre-equalized through a finite impulse response (FIR) filter to pre-compensate for the limited bandwidth and nonlinearity of the transmitter. The processed signal is then loaded into a digital-to-analog converter (DAC) in order to obtain the baseband electrical signal. Afterward, the DAC output signals are amplified by a linear driver and then fed into a modulator for the generation of optical PAM4 signal. The laser can be a vertical cavity surface-emitting laser (VCSEL), a directly modulated laser (DML) or an electro-absorption modulator integrated with distributed feedback laser (EML). A comparison between different kinds of transmitter is summarized in Table 1. Generally, the directly-modulated lasers like VCSEL and DML reach a bandwidth barrier to operate beyond 25 GBaud [54], despite many research efforts made to achieve higher speed transmission [55,56]. EML generally have high bandwidth at the expense of high cost. Since the electrical signals of VCSEL and DML are directly applied to their laser cavity, larger frequency chirps will exist rather than EML, which can induce severe nonlinear distortions and lead to the serious degradation of transmission performance [57,58]. However, the adiabatic chirp of DML causes frequency modulation (FM) of the optical signal, which is able to fundamentally mitigate the first power fading dip incurred by CD [59]. Note that the Mach-Zehnder modulator (MZM) based on

Lithium Niobate ($LiNbO_3$) is out of consideration due to a large footprint and high cost. For optical links below 300 m, the multi-mode fiber (MMF) combined with VSCEL is widely used at present. When the transmission distance increases, the modal dispersion in the MMF will distort the signal and the standard single-mode fiber (SSMF) becomes the common choice.

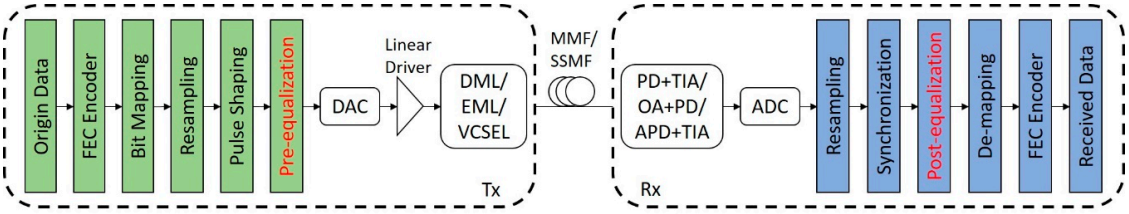

Figure 1. Typical configuration for short-reach PAM4 transmission system.

Table 1. Comparison of different transmitters [54–59].

Tx	Bandwidth	Chirp	Cost	Reach	Fiber	Power Fading	Wavelength (nm)
VSCEL	low	high	low	<300 m	MMF	N/A	Mostly 850
DML	low	high	fair	<80 km	SSMF	low	1310/1550
EML	high	low	high	<80 km	SSMF	high	1310/1550

At the receiver, the signal is directly detected by PD or avalanche photodiode (APD). To improve receiver sensitivity, a TIA is generally cascaded behind to amplify the electrical signal. An alternative solution is using the combination of an optical amplifier (OA) and an optical band-pass filter (OPBF) before PD to amplify received optical signal and remove out-of-band noise. The comparison of different receivers is presented in Table 2, where OA + PD has the highest sensitivity due to the use of high-cost OA. The gain of APD results in relative higher SNR, which makes it more suitable for longer reach links compared to traditional PD [26]. After being processed by an analog-to-digital converter (ADC), the signal is resampled to an expected sampling rate for subsequent steps. Synchronization is achieved to eliminate sampling clock offset (SCO) and depress timing jitter. Then, various DSP techniques are utilized to equalize the received signal for the performance improvement of the transmission system. Finally, after de-mapping and FEC decoding, the received data is obtained and the bit error rate (BER) can be calculated.

Table 2. Comparison of different receivers [1,7,26,39].

Rx	Cost	Footprint	Sensitivity	Reach
PD + TIA	low	low	low	low
APD + TIA	fair	low	fair	fair
OA + PD	high	high	high	high

However, due to the limitation of cost, all transmitters and receivers mentioned above can induce different degree distortions for high-speed PAM4 transmission. Therefore, equalization is one of the most DSP components to eliminate impairments in short-reach optical links. As is shown in Figure 1, the equalization technologies can be utilized both in the transmitter as pre-equalization and in the receiver as post-equalization. The distortions induced by low cost and the different equalization technologies will be introduced specifically in the following sections.

3. Distortions Induced by Low Cost

In short-reach optical links based on PAM4 modulation, the cost is one of the most important factors to be considered for commercial implementation. Low-cost components are highly desired in practical application, while they also bring great challenges and serious distortions such as linear and

nonlinear impairments. In this section, the major distortions induced by low cost will be illustrated in short-reach optical communications.

3.1. Linear Impairments: Limited Bandwidth and Chromatic Dispersion

The high-speed PAM4 system suffers from severe bandwidth limitation due to the consideration of low cost. After bandwidth limited devices, the received signal with low-pass filtering effects can be expressed as:

$$y_k = I_k + \sum_{\substack{n=0 \\ n \neq k}}^{\infty} I_n x_{k-n} + v_k \tag{1}$$

where x_k and y_k is the input signal and output signal at the k-th sampling instant, respectively. The first term I_k represents the desired information symbol while the second term donates the ISI. The last term v_k is the additive Gaussian noise variable at the k-th sampling instant. To investigate the performance impact of bandwidth limitation, a typical measured system frequency response is shown in Figure 2a [60]. The 3 dB bandwidth of the total transmission system is approximately 7.5 GHz, which is far below the required bandwidth for 64 Gbaud PAM4 signal. The attenuation of amplitude frequency is about 15 dB at the Nyquist frequency. In the insets (I) of Figure 3a, it can be observed that the optical eye diagram is confusing, and even four levels of PAM4 signal are unable to be detected. After compensation, a great improvement is achieved in the quality of the eye diagram, which reveals the tremendous influence of limited bandwidth. As shown in the blue part of Figure 2b, the receiver sensitivity penalty is measured as a function of the bandwidth for PAM4 system in simulation [19]. The received optical power at BER = 3.8×10^{-3} for a bandwidth of 35 GHz is employed as reference. It can be seen that approximately 3.3 dB received power is lost as the bandwidth decreases from 35 GHz to 15 GHz. Moreover, the receiver sensitivity penalty increases in speed when the bandwidth limitation becomes severe. The other simulation for PAM4 transmission is depicted in the black part of Figure 2b, where the bandwidths of the components are varied uniformly [61]. The total bit rate is fixed at 96 Gbps, while the 3 dB bandwidths of DAC, modulator, PD and ADC are changed from −30 to 30% simultaneously. The obtained BER performance is degraded as the bandwidth reduces, which confirms that the narrow bandwidth is one of the factors that deteriorate the performance of PAM4 optical links.

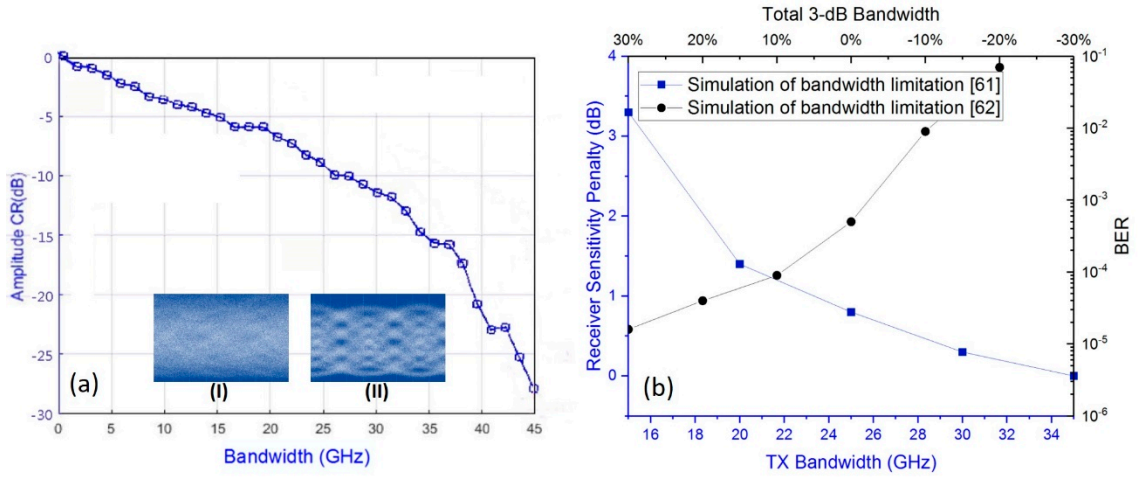

Figure 2. (**a**) Frequency response in band-limited system and eye diagrams (I) before and (II) after bandwidth compensation (redrawn after [60]). (**b**) Effect of bandwidth to system performance (redrawn after [19,61]).

When PAM4 is used in the C-band, the CD tolerance is considered as one key drawback, which critically impairs the high-frequency components of the signal. The typical tolerance to residual

CD in terms of the optical signal-to-noise ratio (OSNR) for PAM4 is shown in Figure 3, where the OSNR penalty is about 1 dB for dispersion within ±100 ps/nm [62]. Meanwhile, the eye diagrams for 56 Gbps PAM4 signal after 0 km and 20 km transmission are shown in Figure 3b,c, respectively. A qualitative comparison between these two eye diagrams reveals that CD brings serious degradation in signal quality.

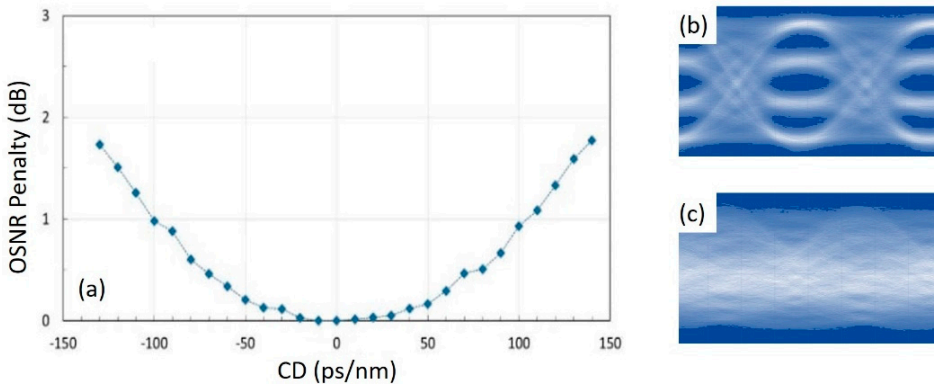

Figure 3. (**a**) Four-level pulse amplitude modulation (PAM4) signaling tolerance on dispersion in terms of optical signal-to-noise ratio (OSNR) penalty (reprinted from [62] with permission from authors). Eye diagrams for 56 Gbps PAM4 signal after (**b**) 0 km and (**c**) 20 km transmission.

3.2. *Nonlinear Impairments*

3.2.1. Nonlinear Devices: Level-Dependent Noise and Level-Dependent Skew

The low cost of devices not only causes the bandwidth limitation but also produces nonlinear distortions like amplitude-dependent noise and level-dependent skew. An example for APD or PD with the optical amplifier is depicted in Figure 4, where different power levels of the PAM4 signal have different distributions of dominant noise [63]. The probability of distributions of regular equally-spaced PAM4 signal after OA + PD and APD receivers are illustrated in Figure 4a,b, respectively. The peaks of probability density represent different noise variances for different levels. From Figure 4c we can notice that high power levels suffer larger noise interference and more symbols cross the decision thresholds, which is consistent with the probability of distributions. Note that the distribution of noise depends on which impairment is dominant, so it is diversified. For instance, the noise of two middle levels could be larger than the noise of two marginal levels considering the nonlinearity of the modulation curve.

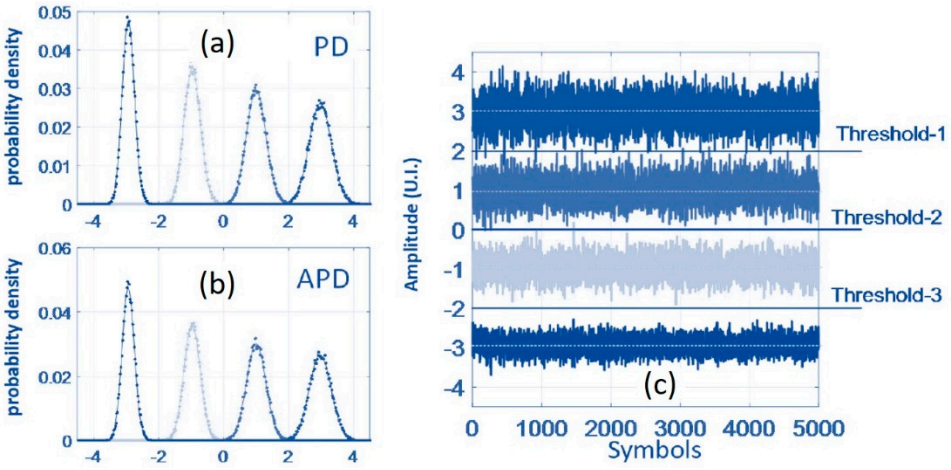

Figure 4. (**a**) The nonlinear probability density distributions of received PAM4 signal for (**a**) OA + PD, and (**b**) APD. (**c**) The waveform of received PAM4 signal after APD (reprinted from [63] with permission from authors).

The level-dependent skew induced by the nonlinear chirp characteristic of modulators can produce significant penalties due to the differences in optimum sampling time for the different level of the eye. As shown in Figure 5a,b, the simulated PAM4 signal without any skew and the simulated 50 Gb/s PAM4 signal using spatial-temporal rate equation modeling [64]. An obvious amplitude-dependent eye can be observed, and hence this inevitably introduces timing impairments. The measured eye diagrams for different signal rates and bias currents of the laser are presented in Figure 5c–f. These figures indicate that the phenomenon of level-dependent skew is more serious under the condition of high-speed and low power consumption, which severely degrades the transmission performance.

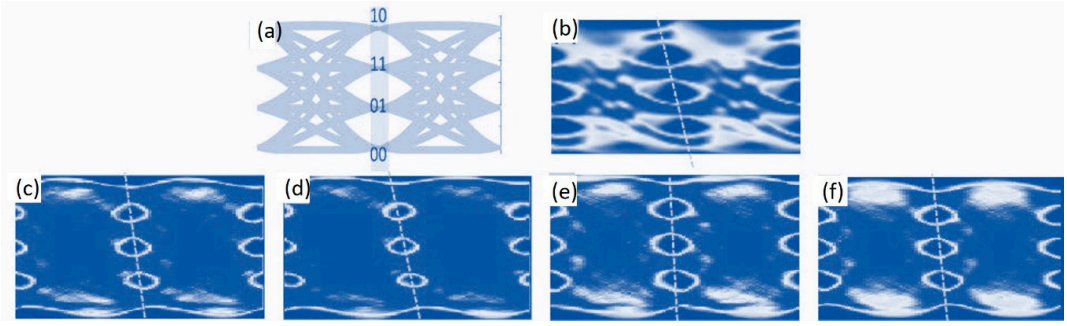

Figure 5. The eye diagrams of (**a**) ideal PAM4 signal; (**b**) simulated PAM4 at 50 Gb/s using spatial-temporal modeling, (**c**) measured 56 Gb/s PAM4 signal when bias current is 5 mA; (**d**) measured 64 Gb/s PAM4 signal when bias current is 5 mA; (**e**) measured 56 Gb/s PAM4 signal when bias current is 7 mA; (**f**) measured 64 Gb/s PAM4 signal when bias current is 7 mA (reprinted from [64] with permission from authors).

3.2.2. Power Fading Effect

Due to the interaction between chromatic CD and direct detection, the induced power-fading effect will produce spectral zeros in the spectrum of the signal, which is the key points to determine transmission distance. Figure 6a–c plots the simulated magnitude response of a 28 Gbaud PAM4 system for various fiber lengths, namely 15 km, 50 km, and 100 km, respectively [65]. It can be clearly seen that the number of spectral zeros changes from none to one and then to three by increasing the transmission distance. Meanwhile, the probability of frequency notches in the high frequency is greater, which proves that the power-fading effect is more severe for high-speed transmission. For experimental demonstrate, the frequency response of the received 25 Gbaud PAM4 signal over 50 km SSMF transmission is depicted in Figure 6d [66]. The first frequency notch can be obviously found around 9 GHz, which indicates that the power fading effect is an inescapable problem in IM/DD system.

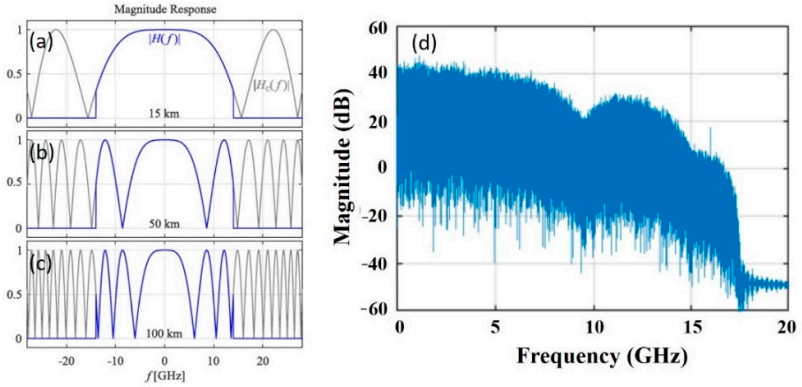

Figure 6. Magnitude responses of a 28 Gbaud PAM4 system after (**a**) 15 km; (**b**) 50 km; (**c**) 100 km in simulation (reprinted from [65] with permission from IEEE). (**d**) Frequency spectrum of the detected 25 Gbaud PAM4 signal over 50 km SSMF transmission (reprinted from [66] with permission from authors).

4. Equalization Technologies

To mitigate the impairments in high-speed PAM4 system mentioned above, various digital equalization technologies have been studied. In this section, we introduce the most popular equalizers, including FFE, DFE, Volterra nonlinear equalizer (VNLE) and machine learning based equalizer, in detail to compensate for these impairments. Moreover, some improved equalization methods are also described to handle specific issues here.

4.1. FFE/DFE

4.1.1. Conventional FFE/DFE

The feed-forward equalizer is an effective method for linear impairments compensation and widely used nowadays. The most basic components of FFE is the finite impulse response (FIR) filter, whose structure is shown in Figure 7a. The output of FIR is expressed as [67]

$$y(k) = \sum_{l=0}^{n-1} h_l x(k-l) \tag{2}$$

where $x(k)$ and $y(k)$ are the input and output signal of FIR at the sampling instant k, respectively. $\mathrm{h} = [h_0 h_1 h_2 \ldots h_{n-1}]$ is the array of tap weights, while n is the number of taps.

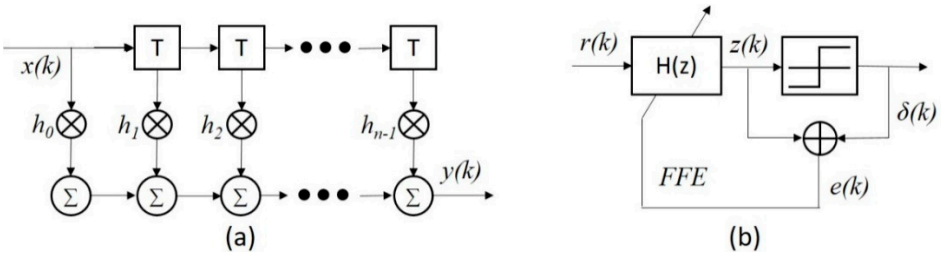

Figure 7. The structure of (**a**) FIR filter: H(z); (**b**) FFE.

Figure 7b depicts the structure of decision-directed FFE, where the FIR filter is noted as $H(z)$. The tap weights can be updated by the zero-forcing (ZF) algorithm, least mean squares (LMS) algorithm, recursive least squares (RLS) algorithm and so on [67–69]. Different convergence algorithms just affect the speed of obtaining optimal tap weights and are not the focus of this review. Here, we only illustrate one of the most common techniques called direct decision LMS (DD-LMS) algorithm. The $(k+1)$-th update of the filter tap weights is given by [68]

$$h(k+1) = h(k) + 2\mu e(k) R(k) \tag{3}$$

where μ is the step size and the error $e(k) = \delta(k) - z(k)$ is between the desired signal $\delta(k)$ and the output signal $z(k)$. The $R(k) = [r(k), r(k-1), r(k-2), \ldots, r(k-n+1)]$ is the vector of the input signal. The FFE can boost the power of high-frequency components that undergo large losses due to the system bandwidth limitations. It should be noted that FFE can operate at symbol rate sampling or higher. Compared with symbol-spaced FFE, the fractionally-spaced FFE which is sampled at several times the symbol rate allows the matched filter to be realized digitally and can take care of phase recovery. In addition, it has a lower residual error at the cost of computational complexity. The destructive effect of the frequency notches is unable to be compensated for easily with an FFE but could be efficiently mitigated using a DFE. Unlike FFE, the input of DFE is the signal after decision, as shown in Figure 8a.

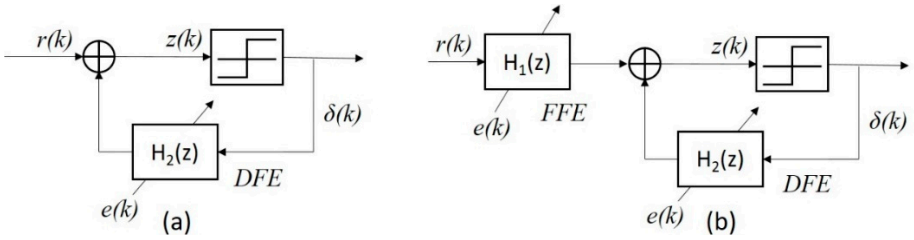

Figure 8. The structure of (**a**) DFE; (**b**) FFE and DFE combined.

In the case of DFE, the signal before decision is calculated by [69]

$$z(k) = r(k) - \sum_{l=0}^{n-1} h_l \delta(k-l) \tag{4}$$

The $(k+1)$th update of the filer tap weights is given by [69]

$$h(k+1) = h(k) + 2\mu e(k) Z(k) \tag{5}$$

where $Z(k) = [z(k), z(k-1), z(k-2), \ldots, z(k-n+1)]$. DFE is usually operated at one sample per symbol. It should be noted that DFE can successfully equalize frequency notches by pole insertion, but it may suffer from error propagation and is unstable due to the decision feedback scheme. Moreover, only post-cursor ISI can be deal with DFE, while the CD-induced channel impulse response contains both pre-cursor and post-cursor. Therefore, the best choice for practical implementation is a combination of an FFE and a DFE, which can be seen from Figure 8b. The FFE and DFE can be placed in the transmitter for pre-compensation or in the receiver for post-compensation [60]. To solve the problem of error propagation, a transmitter-side DFE called Tomlinson-Harashima pre-coding has recently been proposed and investigated in various PAM4 short-reach optical links [70–73]. In addition, many novel equalizers based on conventional FFE/DFE are proposed and investigated to deal with the problems in practical implementation and improve the transmission performance. Next, three recently proposed equalizers including DD-FTN, ID-FFE/ID-DFE, and CR-FFE will be illustrated as examples.

4.1.2. Improved Algorithms Based on FFE/DFE

• DD-FTN

When the FFE tries to amplify the power of high-frequency components to compensate for the low-pass effects, it boosts the noise power at high-frequency components as well. To address this phenomenon, a DD-FTN algorithm is proposed [33] and the principle is shown in Figure 9.

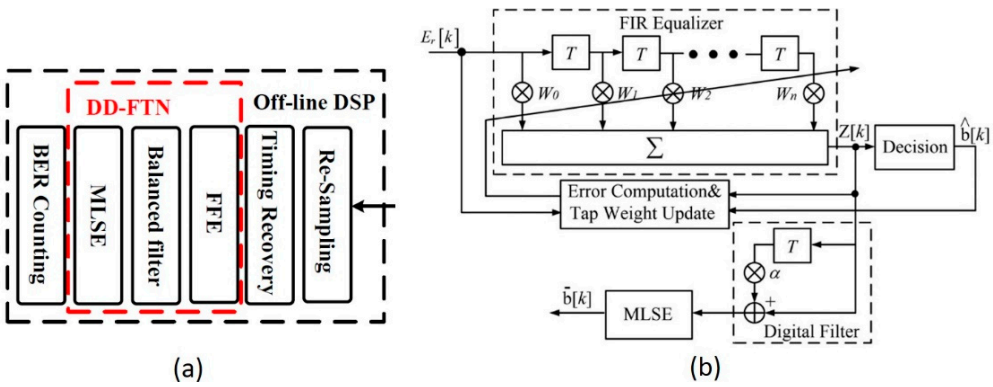

Figure 9. (**a**) The components and (**b**) the structure of DD-FTN (reprinted from [33] with permission from authors and reprinted from [7] with permission from IEEE).

First, the signal after synchronization is equalized by a FFE, adapted by the LMS algorithm. Then, a balanced digital filter is placed behind to suppress the enhanced in-band noise by the equalizer. The transfer function of the balanced filter in z-transform is $H(z) = 1 + \alpha z^{-1}$, where the tap coefficient α is employed to optimize the frequency response of the post filter. Finally, the maximum likelihood sequence estimation (MLSE) is utilized behind to eliminate the strong ISI induced by the balanced filter. Although two more DSP blocks are contained in DD-FTN compared to traditional equalizers, the increase in complexity is relatively small and the overall complexity is not high compared to other DSP techniques.

The BER performance as a function of received optical power for 112 Gbps PAM4 signal after 2 km SSMF transmission is depicted in Figure 10a [33]. With conventional FFE, the enhanced noise significantly degrades the system performance and a BER floor at 5×10^{-2} can be observed. By using DD-FTN, the noise enhancement is effectively mitigated by the balanced filter and the induced ISI can be processed by the MLSE. The performance is improved and the BER can reach 3×10^{-4} when received power is −7.1 dBm. Figure 10b shows the BER performance versus received optical power for 140 Gbit/s PAM-4 system after back-to-back transmission [35]. It can be found that the traditional FFE updated by DD-LMS exhibits the worst performance, while the BER can reach the hard decision FEC (HD-FEC) threshold of 3.8×10^{-3} with DD-FTN. Therefore, DD-FTN can make a big difference in enhanced noise mitigation.

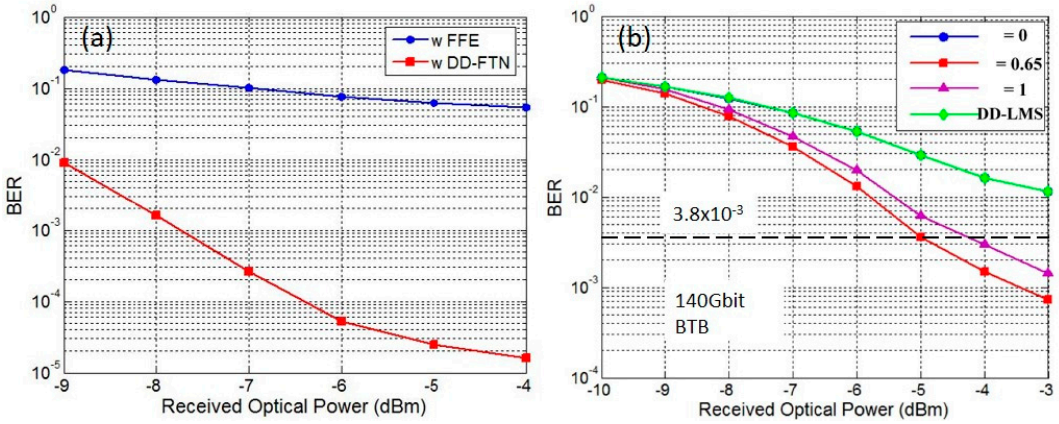

Figure 10. (**a**) The bit error rate (BER) performance versus received optical power for 112 Gbps PAM4 signal after 2 km SSMF transmission (reprinted from [33] with permission from authors). (**b**) The BER performance versus received optical power for different tap coefficient of balanced filter for 140 Gbit/s PAM4 system after back-to-back transmission (reprinted from [35] with permission from IEEE).

• ID-FFE/ID-DFE

In C-band transmission, low-cost modulator like DML will introduce an additional impairment due to the interaction between frequency chirp and chromatic dispersion. Recently, a low complexity intensity directed equalizer based on FFE and DFE is proposed to suppress the chirp induced distortions. Different from the traditional FFE/DFE that utilizes one set of coefficients, the proposed algorithm first divides the symbol into different sets according to its intensity level, as shown in Figure 11a [37]. Then the coefficients of different groups are applied accordingly. Four sets of coefficients for PAM4 symbol are selected according to the three thresholds for ID-FFE and four levels for ID-DFE. After classification, the desired tap coefficients from different sets are used and the following procedures are the same as the traditional FFE/DFE. In terms of complexity, only a few simple decision circuits are added to the original FFE/DFE and the complexity increment is negligible considering the operations of multiplication in the equalizer.

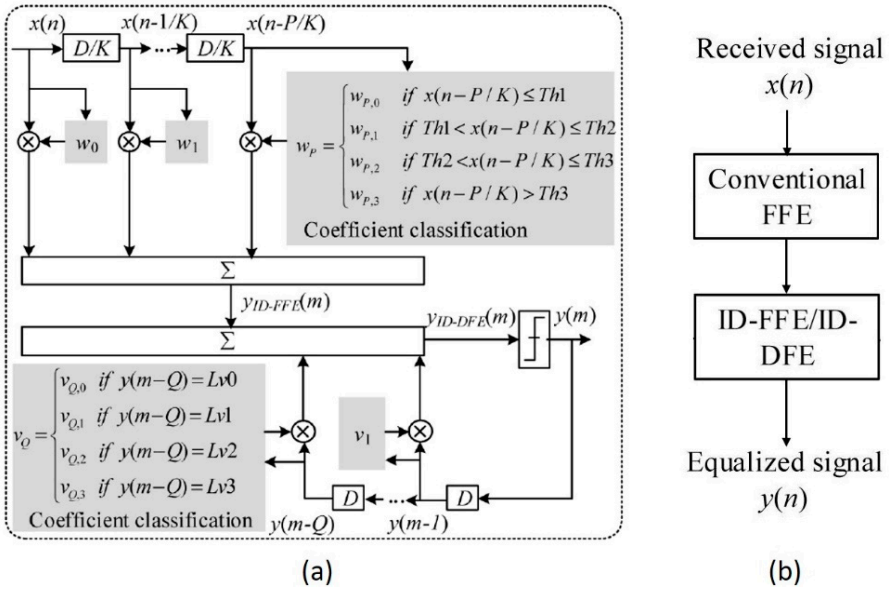

Figure 11. (**a**) The detailed structure of (P-1)-tap ID-FFE and Q-tap ID-DFE. (**b**) The block diagram of the pre-FFE + ID-FFE/ID-DFE (reprinted from [37] with open access from OSA).

The effectiveness of ID-FFE/ID-DFE greatly depends on the accuracy of the decision in the classification. Thus, a conventional FFE is employed to equalize the severe impairments and enhance the decision accuracy before the intensity directed equalizer as shown in Figure 11b.

The BER performance versus the received optical power is shown in Figure 12 [37]. Compared with the FFE case, of which the BER is 9×10^{-3}, the ID-FFE/ID-DFE reaches 2×10^{-3}. When the pre-FFE is used before ID-FFE/ID-DFE, the performance is improved by almost an order of magnitude and the BER reduce to 2.6×10^{-4}. From the received eye diagrams of ID-FFE with and without pre-FFE, we observe that the pre-FFE can completely suppress the residual eye skewing effect of the ID-FFE and dramatically remove the ISI. When the transmission distance increase to 43 km, only the ID-FFE/ID-DFE assisted by pre-FFE can reach a BER of 3.6×10^{-3} below the HD-FEC. Therefore, the chirp of the modulator can be well addressed by the novel proposed ID-FFE/ID-DFE.

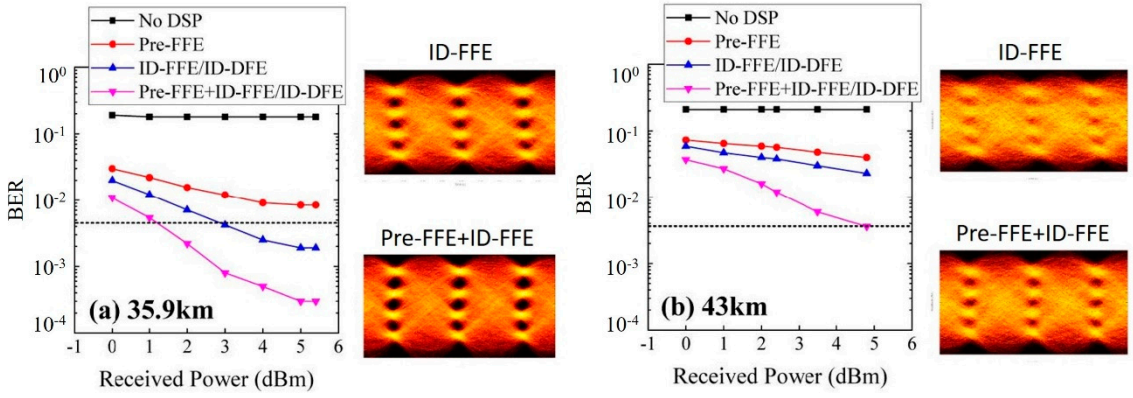

Figure 12. The BER performance of 56 Gbps PAM4 signal (**a**) after 35.9 km transmission and (**b**) after 43 km transmission (reprinted from [37] with open access from OSA).

• CR-FFE

The problem of incompatible prerequisites between impairment equalization and clock recovery also reduces the performance of PAM4 transmission [74]. A joint clock recovery and feed-forward equalization algorithm is proposed recently, which estimates timing error based on the difference

between two tap coefficients of T/2-spaced FFE. The proposed algorithm can eliminate the ISI induced by linear impairments and track large sampling clock offset (SCO) simultaneously.

The structure of the CR-FFE is plotted in Figure 13, where we notice that the timing error is derived from the difference between two tap coefficients [39]. For the comparison of complexity, the timing error of CR-FFE is calculated by one time subtraction, while the conventional CR algorithm needs an additional multiplication. Considering the total multiplication operations, the computational complexity of CR-FFE is similar to or slightly lower than that of the original scheme.

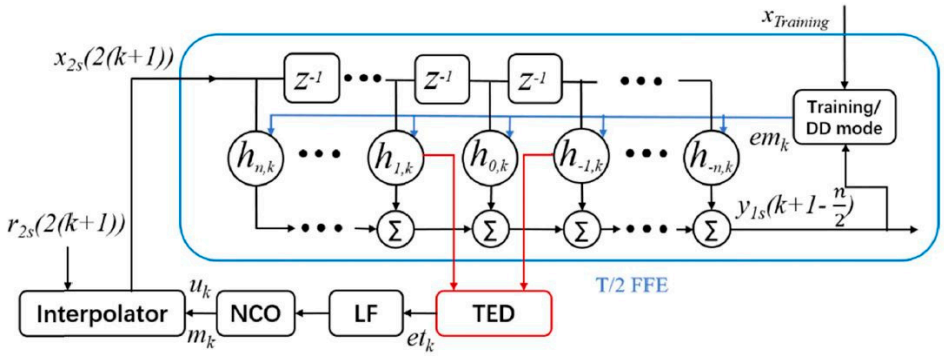

Figure 13. The structure of proposed joint clock recovery and FFE (CR-FFE) (reprinted from [39] with open access from OSA).

The BER performance of CR-FFE over different SCO is studied as shown in Figure 14a [39]. The traditional clock recovery cascaded by FFE (noted as scheme II) cannot counteract large SCO, while the CR-FFE (noted as scheme III) can ensure stable and reliable performance as SCO increase from 0 to 1000 ppm. From Figure 14b,c, we observe that the two tap coefficients for timing error detection are basically equal and the fractional interval has a stable changing process, which indicates that clock recovery and equalization are accomplished simultaneously after 40 km transmission when SCO reaches 1000 ppm. Therefore, the CR-FFE can solve the problem of incompatible prerequisites between impairment equalization and clock recovery, and provide significant system performance improvement for PAM4 transmission.

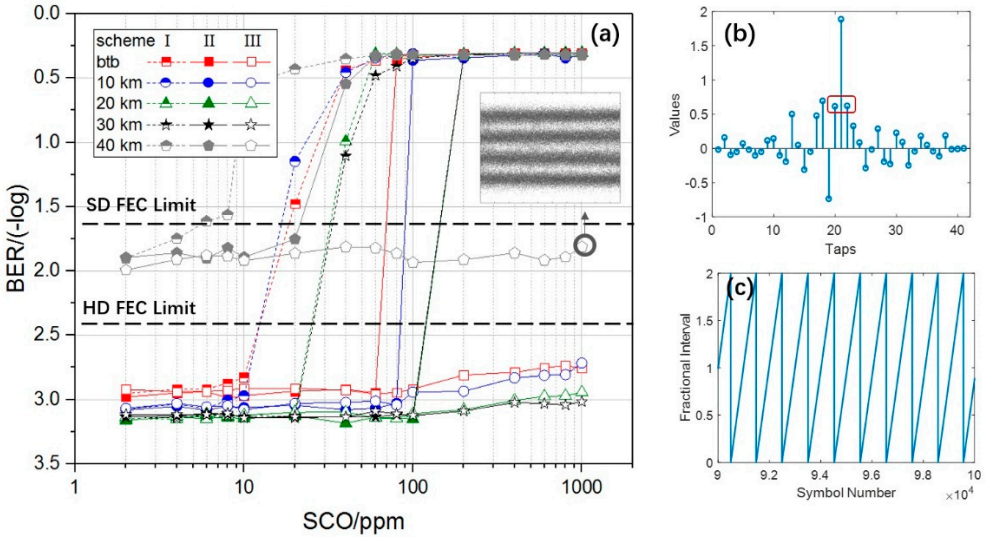

Figure 14. (**a**) The BER performance vs. sampling clock offset at received optical power of –8 dBm for 50 Gbps PAM4 signal; (**b**) the tap weights and (**c**) fractional interval of proposed CR-FFE after 40 km transmission when sampling clock offset is 1000 ppm (reprinted from [39] with open access from OSA).

4.2. VNLE

Thanks to FFE and DFE, the linear impairments can be efficiently eliminated. However, the residual nonlinear distortion mainly induced by the nonlinearity of devices and square-law detection can also severely impact the transmission performance of the PAM4 system. One of the most popular equalization techniques is VNLE, whose structure is shown in Figure 15. Note that the VNLE can be implemented based on FFE or DFE and we focus on FFE based VNLE in this paper. Considering the exponential growth of computational complexity, the third-order VNLE is introduced here.

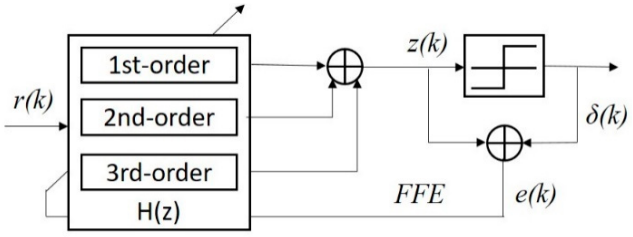

Figure 15. The structure of Volterra nonlinear equalizer (VNLE).

The output of VNLE is expressed as [75]

$$z(k) = \sum_{l=0}^{n_1-1} h_l x(k-l) + \sum_{l=0}^{n_2-1}\sum_{i=0}^{l} h_{l,i} x(k-l)x(k-i) + \sum_{l=0}^{n_3-1}\sum_{i=0}^{l}\sum_{j=0}^{i} h_{l,i,j} x(k-l)x(k-i)x(k-j) \quad (6)$$

where h_l, $h_{l,i}$ and $h_{l,i,j}$ are the tap weights of 1st-order, 2nd-order and 3rd-order kernels, respectively. $x(k)$ is the input signal of FIR in VNLE at the sampling instant k. In addition, n_1, n_2 and n_3 respectively represent the number of taps for the linear part, 2nd-order nonlinear part and 3rd-order nonlinear part. Generally, the linear impairments of the PAM4 system and the self-phase modulation (SPM) of SSMF can be successfully eliminated by the first and third-order kernels of VF, while the second-order kernels are utilized to compensate the nonlinearity of devices such as modulator and PD. The kernel coefficients are commonly updated by LMS algorithm considering complexity. To simplify the convergence procedure, the kernels of each order are evolved at different speeds [75], which can be depicted as a gradient vector $\mu = [\mu_1, \mu_2, \mu_3]$. However, there is no clear procedure on how to set the values of this vector.

While limited by the high computation complexity of fully-connected VNLE, it is not practical to be implemented directly in the real applications. Various methods have been proposed to reduce the computational complexity of VNLE and the interested readers can refer to [76–80] for a detailed discussion on this topic. Taking modified Gram-Schmidt orthogonal decomposition as an example, the performance of sparse VNLE is described as shown in Figure 16 [31]. The dependence of the BER on the back-to-back system without VNLE, and with VNLE or sparse VNLE are compared. As is shown, the required ROP at the FEC threshold is decreased by 0.7 dB for the VNLE. When sparse VNLE is employed, the increase in the ROP is less than 0.2 dB compared to VNLE. Figure 6b plots the dependence of the BER on the ROP for 10 km and 20 km transmission. No penalties are observed relative to the back-to-back system. Therefore, the sparse VNLE can maintain basically the same performance with a reduction of computational complexity, which is an excellent optimization for VNLE.

4.3. Equalization Based on Machine Learning

Machine learning (ML) is the scientific study of algorithms and statistical models that computer systems use to effectively perform a specific task without using explicit instructions, which was coined in 1959 by Arthur Samuel [81]. Recently, machine learning algorithms have been utilized to process optical communications and achieve distinguished performance [82–86]. Some DSP techniques based on machine learning including SVM and NN are described in this section for PAM4 optical links.

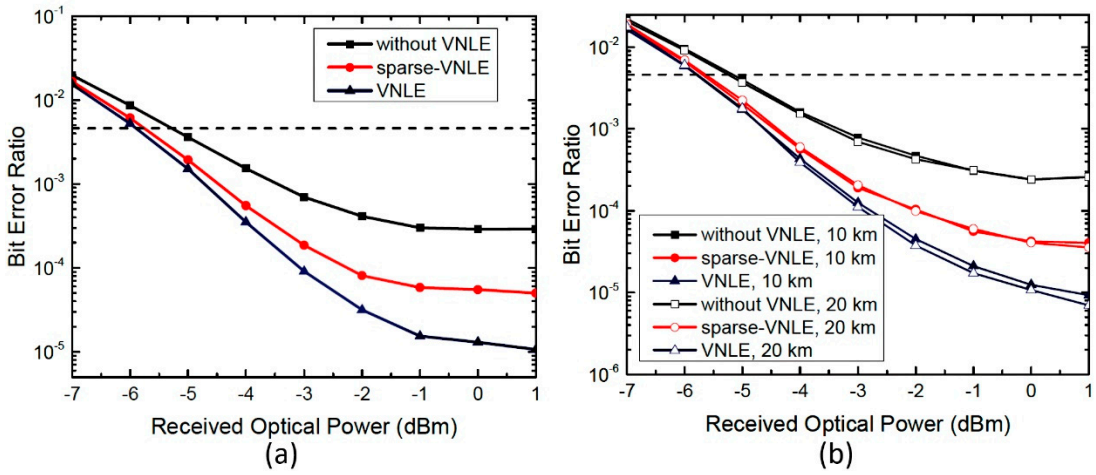

Figure 16. (**a**) BER vs. received optical power for a back-to-back system. (**b**) BER vs. received optical power for 10 km and 20 km transmission (reprinted from [31] with permission from authors).

4.3.1. Support Vector Machine

The basic SVM classifier is a two-class classifier and its training process can be described as finding the maximum edge hyperplane to define the decision function of the classifier. The concept of basic SVM classifier is shown in Figure 17a, where the margin means the minimum distance of all samples to the hyper-plane [40]. To solve this convex quadratic programming of optimization target in SVM, the sequential minimal optimization (SMO) algorithm [87] can be used.

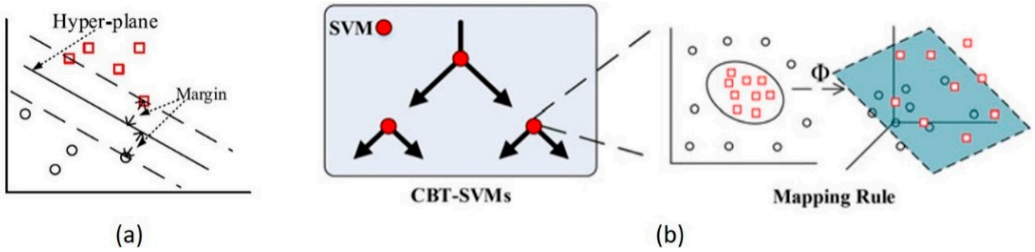

Figure 17. (**a**) Basic SVM classifier. (**b**) Complete binary tree structure multi-classes SVMs and mapping rule for PAM4 signal where the black circle and the red square represent two categories (reprinted from [40] with permission from IEEE).

Note that PAM4 cannot be de detected directly by the basic SVM classifier. Thus, a proposed complete binary tree (CBT) structure multi-classes SVMs method is utilized as depicted in Figure 17b. It can be seen that two layers are contained in the tree, where the first layer classifies the first bit of PAM4 signal, and the second layer classifies the last bit. Although the wrong decision in the high layer will be retained to the next layers, a significant improvement in performance for PAM4 system can still be expected.

The BER curves of the 40 Gbps and 50 Gbps PAM4 signal are shown in Figure 18a,b, respectively [42]. Using the proposed CBT-SVMs, significant receiver sensitivity reduction of 2.99 dB and 4.68 dB in optical B2B and 2 km SMF transmission can be obtained for 40 Gbps PAM4 system. Moreover, for 50 Gbps PAM4 modulation, it provides 3.59 dB and 3.63 dB received power tolerance compared with the hard decision. Therefore, the SVM algorithm shows outstanding performance in nonlinear impairment mitigation and could be a potential choice for future PAM4 optical links.

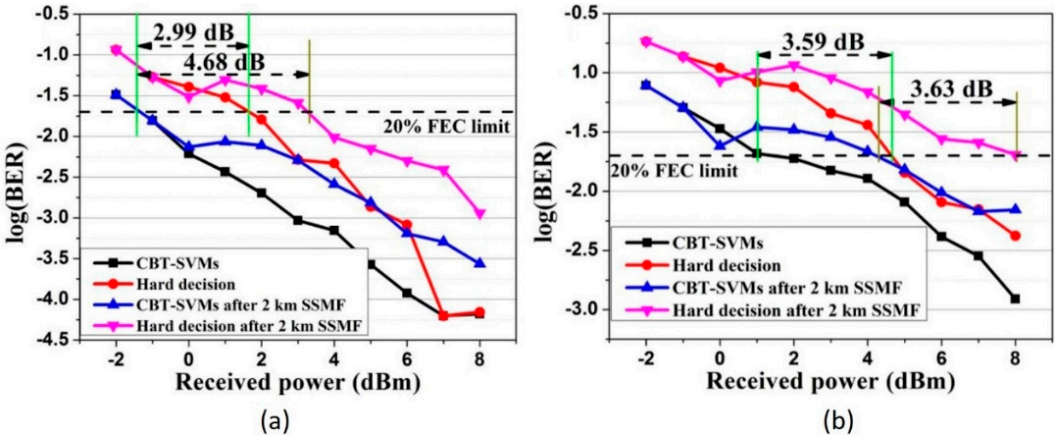

Figure 18. BER curves for (**a**) 40 Gbps and (**b**) 50 Gbps PAM4 signal using CBT-SVMs (reprinted from [42] with permission from IEEE).

4.3.2. Neural Network

The neural network (NN) is computational model loosely inspired by its biological counterparts [88]. In recent years, it has been proposed to mitigate the nonlinear impairments in optical communication system [89–91]. For short-reach PAM4 optical links, various research concerning the NN method has been performed to improve transmission performance [43–53]. The schematic of NN based nonlinear signal processing is presented in Figure 19a, where the leftmost part consists of a set of neurons representing the input features and the rightmost part is a non-linear activation function [48]. In the middle, a weighted linear summation is employed to represent connections between neurons. Figure 19b shows a two-layer neural network to classify PAM4 signals. Rectified Linear Units (ReLU), as indicated in the inset of Figure 19b, is always applied as the activation function. Compared with sigmoid function or Tanh function, it is more like a real neuron in our body and results in much faster training. A softmax function is commonly selected as the activation function for the output layer. The output of the softmax function is the class with the highest probability.

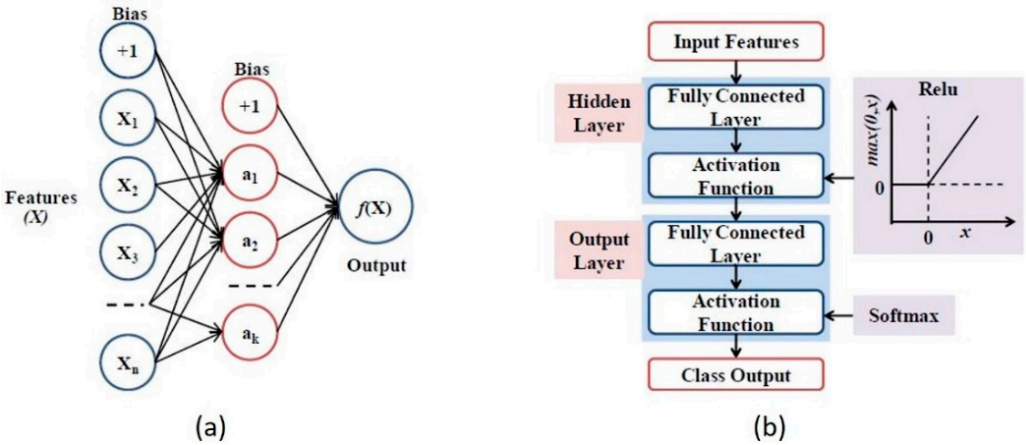

Figure 19. (**a**) Schematic of neural network (NN) based nonlinear signal processing for a hidden layer and (**b**) simple structure of two-layer neural network (reprinted from [48] with permission from authors).

An example for BER performance of NN is shown in Figure 20a [49]. Thanks to the NN method, about one order of magnitude is decrease compared to the BER with VNLE after 60 km transmission. Figure 20b shows the BER performance versus OSNR after 80 km SSMF. The required OSNRs to reach the FEC threshold for VNLE and NN are 39 dB and 35.5 dB, respectively. Thus, we can conclude that

compared to conventional equalizers, a better BER performance can be achieved using the NN method, which is an attractive solution for short-reach PAM4 optical links.

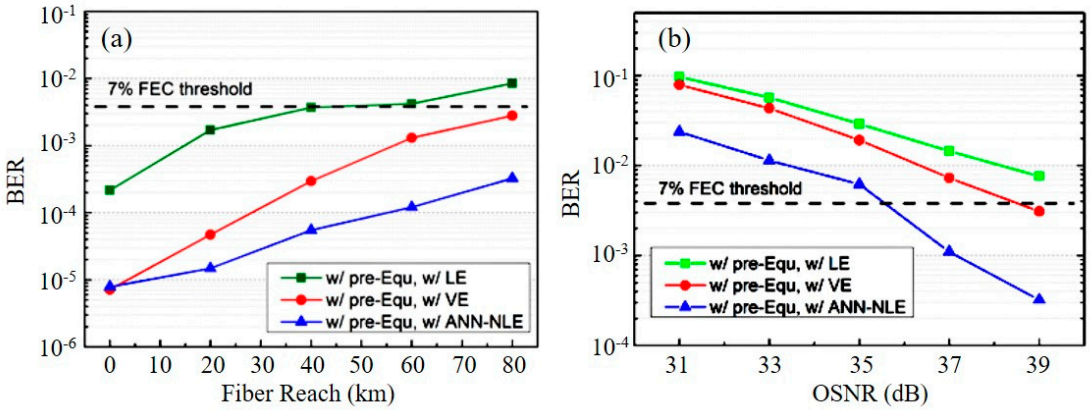

Figure 20. (**a**) BER vs. fiber length with NN for 112 Gbps SSB-PAM4 transmission. (**b**) BER vs. OSNR after 80 km dispersion uncompensated SSMF (reprinted from [49] with open access from OSA).

4.4. Summary of Recent Work

Various equalization technologies mentioned above are summarized and compared as shown in Table 3. The FFE/DFE is widely used in short-reach PAM4 optical links due to simple architecture and low complexity, however, it can only eliminate the linear ISI induced by bandwidth limitation and CD. In [26], a single-channel 56 Gbit/s PAM4 optical transmission over 60 km is experimentally demonstrated with receiver sensitivities of −19.9 dBm using 35 taps FFE. Meanwhile, with the help of 17 taps FFE, the 40 km error-free transmission is achieved for 106 Gbit/s PAM4 using APD receiver [27]. The THP is a transmitter-side DFE without suffering from error-propagation, which is proposed recently to resist against power fading and bandwidth limitation. For the first time, the THP is applied to 100 Gbit/s FTN PAM4 transmission over 40 km through a 20 GHz low-pass channel [72]. With similar or a low addition of complexity, the novel DD-FTN, ID-FFE/ID-DFE and CR-FFE can compensate for the weakness of conventional linear equalizers and achieve better performance for specific issues. In [35], the DD-FTN is experimentally demonstrated for a 140 Gbit/s PAM4 signal over 20 km transmission with a receiver sensitivity of −5.5 dBm. K. Zhang et al. firstly demonstrate a C-band 56 Gbit/s PAM4 system over 43 km transmission with the proposed ID-FFE/ID-DFE [37]. In [39], the CR-FFE resist SCO up to 1000-ppm after 40 km transmission for 50 Gbit PAM4 system based on 10 GHz DML. While bandwidth limitation can be efficiently compensated for by using FFE/DFE, the nonlinearity of devices is difficult to eliminate effectively. VNLE is the most popular nonlinear equalization while the high computational complexity can be reduced by removing the less important kernels. Using 1722 taps VNLE, the C-band 2 × 56 Gbit/s PAM4 transmission over 100 km is experimentally demonstrated in [92]. A sparse VNLE with half computational complexity achieves similar performance for 2×64 Gbit/s PAM4 transmission over 70 km SSMF using 18 GHz DML [93]. As for machine learning algorithms, SVM and NN including artificial NN (ANN), deep NN (DNN), and convolutional NN (CNN) are the mainstream to further eliminate nonlinear distortions of PAM4 optical links with higher complexity. When the SVM is applied to PAM4 signal, sensitivity gain of 2.5 dB is obtained for 60 Gbit/s VCSEL-MMF short-reach optical links [40]. Yang et al. experimentally demonstrate a C-band 4 × 50 Gbit/s PAM4 transmission over 80 km SSMF employing a radial basis function ANN [44]. In [46], with the help of CNN, a 112 Gbit/s PAM4 transmission over 40 km SSMF is accomplished and the BER performance outperforms traditional VNLE. For more complicated DNN, the BER of 4.41×10^{-5} is obtained for a 64 Gbit/s PAM4 transmission over 4 km MMF based on 850 nm VCSEL [47]. Note that some equalization methods such as look-up table (LUT) are not mentioned in this paper due to less implementation.

Table 3. Equalization technologies for short-reach PAM4 optical links.

Equalization	Distortion	Rate (Gbps)	Reach (km)	Wavelength (nm)	FEC	Tx	Rx	Ref.
FFE/DFE	bandwidth limitation & CD	56	60	1295.13	3.8×10^{-3}	EML	APD + TIA & PD + TIA	[26]
FFE/DFE	bandwidth limitation & CD	106	40	1309.49	2×10^{-4}	EML	APD	[27]
FFE/DFE	bandwidth limitation & CD	112	40	1314	1×10^{-3}	EML	PD + TIA	[28]
THP	bandwidth limitation & power fading	100	40	1300	4×10^{-3} & 2×10^{-4}	EML	PD + TIA	[72]
DD-FTN	enhanced noise	140	20	1296.2	3.8×10^{-3}	EML	PD + TIA	[35]
ID-FFE/ ID-DFE	chirp of modulator	56	43	N/A	3.8×10^{-3}	DML	PD	[37]
CR-FFE	clock offset with CD	50	40	1549.39	2×10^{-2}	DML	OA + PD	[39]
VNLE	nonlinearity	56	100	1549.81	3.8×10^{-3}	DML	OA + PD	[92]
VNLE	nonlinearity	56	70	1311.89	3.8×10^{-3}	DML	OA + PD	[93]
SVM	nonlinearity of VSCEL	60	0.05	850	3.8×10^{-3}	VSCEL	PD	[40]
SVM	level-dependent skew	50	20	1551	1×10^{-3} & 2×10^{-4}	DML	PD	[41]
ANN	nonlinearity of DML	20	18	1310	3.8×10^{-3}	DML	PD	[43]
ANN	nonlinearity	50	80	1551.35	3.8×10^{-3}	DML	OA + PD	[44]
CNN	nonlinearity	56	25	N/A	3.8×10^{-3}	DML	APD	[45]
CNN	nonlinearity	112	40	1293	2×10^{-4}	EML	PD + TIA	[46]
DNN	nonlinearity	64	4	850	2×10^{-4}	VSCEL	PD + TIA	[47]
DNN	nonlinearity	50	80	1551.35	1×10^{-3}	DML	OA + PD	[48]

At present, the standard to evaluate the equalization technologies is considering both the performance improvement and the computational complexity. The high complexity will occupy massive resources for computation, thus increasing the computational cost. The score to judge the equalization technologies can be described as:

$$\text{score} = \frac{a * \text{performance improvement}}{b * \text{computational cost}} \tag{7}$$

where a and b are the influence factors of performance improvement and computational cost, respectively. The comparison of the computational complexity and performance improvement for different equalization technologies is summarized in Table 4. Note that the main limited factor for the short-reach PAM4 system is the cost, and the goal for equalization technologies is to achieve better performance at the same computation cost. As is shown in Table 4, the SVM an NN have a higher complexity than conventional equalization, although the performance can be significantly improved. However, the computation cost is getting lower as the continuous development of the integrated circuit. So, from the long-term point of view, the equalization based on machine learning algorithms will play an increasingly important role for short-reach PAM4 optical links.

Table 4. Comparison of the computational complexity and performance improvement for different equalization technologies.

Equalization Technologies	FFE/DFE	DD-FTN	ID-FFE/ ID-DFE	CR-FFE	VNLE	Sparse VNLE	SVM	NN
Computational Complexity	low	fair	low	low	high	fair	high	high
Performance Improvement	low	fair	fair	fair	high	high	high	high

5. Conclusions and Perspective

In this paper, we have reviewed various equalization technologies for short-reach PAM4 optical links. A typical system configuration is presented and the comparisons among different transmitters and receivers are introduced. Different distortions including linear impairments, device nonlinearity and power fading effect are described, which are induced by low-cost components and need to be mitigated by pre- and post-equalization. The conventional equalizers, including FFE and DFE, are illustrated to eliminate the linear impairments such as bandwidth limitation and chromatic dispersion, while the nonlinear distortions are compensated for by conventional VNLE and sparse VNLE. The machine learning algorithms like SVM and NN are proposed to further mitigate severe nonlinear distortion and achieve significant performance improvement. Finally, a summary is given for different equalization technologies and a standard for the evaluation of equalizers is defined to consider both performance improvement and computational complexity. Additionally, as the cost of computation constantly decreases, equalization technologies based on machine learning may become the mainstream technology for next-generation short-reach PAM4 transmission.

Author Contributions: This paper was mainly wrote by H.Z. and Y.L. (Yan Li) Y.L. (Yuyang Liu) provided the idea and J.W. supervised overall project. L.Y., C.G., W.L., J.Q., H.G., X.H., Y.Z. and J.W. contributed to the reviewing and editing of the manuscript.

Funding: This paper is partly funded by National Natural Science Foundation of China (NSFC) (61875019, 61675034, 61875020, 61571067); The Fund of State Key Laboratory of IPOC (BUPT); The Fundamental Research Funds for the Central Universities.

Acknowledgments: We would like to thank the unknown reviewers that helped improve this manuscript with their valuable feedback.

Conflicts of Interest: The authors declare no conflict of interest.

Abbreviations

Acronyms		Acronyms	
ADC	Analog-to-digital converter	APD	Avalanche photodiode
BER	Bit error rate	CAP	Carrier-less amplitude and phase modulation
CBT	Complete binary tree	CD	Chromatic dispersion
CR	Clock recovery	DAC	Digital-to-analog converter
DCI	Data center interconnects	DD	Direct detection
DFE	Decision feedback equalizer	DML	Directly modulated laser
DMT	Discrete multi-tone	DSP	Digital signal processing
EML	Electro-absorption modulated lasers	FEC	Forward error correction
FFE	Feed-forward equalizer	FTN	Faster than nyquist
HD	Hard decision	ID	Intensity directed
IM	Intensity modulation	ISI	Inter-symbol interference
KK	Kramers-Kronig	LMS	Least mean squares
MLSE	Maximum likelihood sequence estimation	ML	Machine learning
MMF	Multi-mode fiber	MZM	Mach-Zehnder modulator
NN	Neural network	OA	Optical amplifier
OPBF	Optical band-pass filter	OSNR	Optical signal-to-noise ratio
PAM4	Four-level pulse amplitude modulation	PD	Photodiodes
PRBS	Pseudorandom binary sequence	QAM	quadrature amplitude modulation
ReLU	Rectified Linear Units	RLS	Recursive least squares
SCO	Sampling clock offset	SMMF	Standard single-mode fiber
SMO	Sequential minimal optimization	SPM	Self-phase modulation
SVM	Support vector machine	TIA	Trans-impedance amplifiers
VCSEL	Vertical cavity surface-emitting laser	VNLE	Volterra nonlinear equalizer
VR	virtual reality	ZF	Zero-forcing

References

1. Chen, Q.; Bahadori, M.; Glick, M.; Rumley, S.; Bergman, K. Recent advances in optical technologies for data centers: A review. *Optica* **2018**, *11*, 1354–1370. [CrossRef]
2. Cisco Visual Networking. *The Zettabyte Era—Trends and Analysis*; Cisco White Paper: San Jose, CA, USA, 2017.
3. Zhong, K.; Zhou, X.; Wang, Y.; Gui, T.; Yang, Y.; Yuan, J.; Wang, L.; Chen, W.; Zhang, H.; Man, J.; et al. Recent Advances in Short Reach Systems. In Proceedings of the Optical Fiber Communication Conference (OFC), Los Angeles, CA, USA, 19–23 March 2017; p. Tu2D.7.
4. Plant, D.V.; Morsy-Osman, M.; Chagnon, M. Optical communication systems for datacenter networks. In Proceedings of the Optical Fiber Communications Conference (OFC), Los Angeles, CA, USA, 19–23 March 2017; pp. 1–47.
5. Cartledge, J.C.; Karar, A.S. 100 Gb/s Intensity Modulation and Direct Detection. *J. Lightw. Technol.* **2014**, *16*, 2809–2814. [CrossRef]
6. Wei, J.; Cheng, Q.; Penty, R.V.; White, I.H.; Cunningham, D.G. 400 Gigabit Ethernet using advanced modulation formats: Performance, complexity, and power dissipation. *Commun. Mag.* **2015**, *2*, 182–189. [CrossRef]
7. Zhong, K.; Zhou, X.; Huo, J.; Yu, C.; Lu, C.; Lau, A.P.T. Digital signal processing for short-reach optical communications: A review of current technologies and future trends. *J. Lightw. Technol.* **2018**, *2*, 377–400. [CrossRef]
8. Xu, X.; Zhou, E.; Liu, G.N.; Zuo, T.; Zhong, Q.; Zhang, L.; Bao, Y.; Zhang, X.; Li, J.; Li, Z. Advanced modulation formats for 400-Gbps short-reach optical inter-connection. *Opt. Express* **2015**, *1*, 492–500. [CrossRef] [PubMed]
9. Lyubomirsky, I.; Ling, W.A. Advanced Modulation for Datacenter Interconnect. In Proceedings of the Optical Fiber Communications Conference (OFC), Anaheim, CA, USA, 20–24 March 2016; pp. 1–3.
10. Eiselt, N.; Griesser, H.; Wei, J.; Hohenleitner, R.; Dochhan, A.; Ortsiefer, M.; Eiselt, M.H.; Neumeyr, C.; José Vegas Olmos, J.; Monroy, I.T. Experimental Demonstration of 84 Gb/s PAM-4 Over up to 1.6 km SSMF Using a 20-GHz VCSEL at 1525 nm. *J. Lightw. Technol.* **2017**, *8*, 1342–1349. [CrossRef]
11. Sadot, D.; Dorman, G.; Gorshtein, A.; Sonkin, E.; Vidal, O. Single channel 112Gbit/sec PAM4 at 56Gbaud with digital signal processing for data centers applications. *Opt. Express* **2015**, *2*, 991–997. [CrossRef] [PubMed]
12. Tao, L.; Wang, Y.; Xiao, J.; Chi, N. Enhanced performance of 400 Gb/s DML-based CAP systems using optical filtering technique for short reach communication. *Opt. Express* **2014**, *24*, 29331–29339. [CrossRef]
13. Shi, J.; Zhang, J.; Li, X.; Chi, N.; Chang, G.; Yu, J. 112 Gb/s/λ CAP Signals Transmission over 480 km in IM-DD System. In Proceedings of the Optical Fiber Communications Conference (OFC), San Diego, CA, USA, 11–15 March 2018; pp. 1–3.
14. Zhang, L.; Zuo, T.; Mao, Y.; Zhang, Q.; Zhou, E.; Liu, G.N.; Xu, X. Beyond 100-Gb/s Transmission Over 80-km SMF Using Direct-Detection SSB-DMT at C-Band. *J. Lightw. Technol.* **2016**, *2*, 723–729. [CrossRef]
15. Sun, L.; Du, J.; Wang, C.; Li, Z.; Xu, K.; He, Z. Frequency-resolved adaptive probabilistic shaping for DMT-modulated IM-DD optical interconnects. *Opt. Express* **2019**, *9*, 12241–12254. [CrossRef]
16. Zhu, Y.; Zou, K.; Chen, Z.; Zhang, F. 224 Gb/s Optical Carrier-Assisted Nyquist 16-QAM Half-Cycle Single-Sideband Direct Detection Transmission over 160 km SSMF. *J. Lightw. Technol.* **2017**, *9*, 1557–1565. [CrossRef]
17. Chen, X.; Antonelli, C.; Chandrasekhar, S.; Raybon, G.; Mecozzi, A.; Shtaif, M.; Winzer, P. Kramers–Kronig Receivers for 100-km Datacenter Interconnects. *J. Lightw. Technol.* **2018**, *1*, 79–89. [CrossRef]
18. Mecozzi, A.; Antonelli, C.; Shtaif, M. Kramers–Kronig coherent receiver. *Optica* **2016**, *11*, 1220–1227. [CrossRef]
19. Zhong, K.; Zhou, X.; Gui, T.; Tao, L.; Gao, Y.; Chen, W.; Man, J.; Zeng, L.; Lau, A.P.T.; Lu, C. Experimental study of PAM-4, CAP-16, and DMT for 100 Gb/s short reach optical transmission systems. *Opt. Express* **2015**, *2*, 1176–1189. [CrossRef] [PubMed]
20. Shi, J.; Zhang, J.; Zhou, Y.; Wang, Y.; Chi, N.; Yu, J. Transmission Performance Comparison for 100-Gb/s PAM-4, CAP-16, and DFT-S OFDM With Direct Detection. *J. Lightw. Technol.* **2017**, *23*, 5127–5133. [CrossRef]
21. Yekani, A.; Rusch, L.A. Interplay of Bit Rate, Linewidth, Bandwidth, and Reach on Optical DMT and PAM with IMDD. *Trans. Commun.* **2019**, *4*, 2908–2913. [CrossRef]

22. Houtsma, V.; Veen, D. Optical Strategies for Economical Next Generation 50 and 100G PON. In Proceedings of the Optical Fiber Communications Conference (OFC), San Diego, CA, USA, 3–7 March 2019; p. M2B.1.
23. Nesset, D. PON roadmap. *J. Opt. Commun. Netw.* **2017**, *1*, A71–A76. [CrossRef]
24. Zhang, K.; Zhuge, Q.; Xin, H.; Xing, Z.; Xiang, M.; Fan, S.; Yi, L.; Hu, W.; Plant, D.V. Demonstration of 50Gb/s/λ Symmetric PAM4 TDM-PON with 10G-class Optics and DSP-free ONUs in the O-band. In Proceedings of the Optical Fiber Communications Conference (OFC), San Diego, CA, USA, 11–15 March 2018; pp. 1–3.
25. Ethernet Task Force. IEEE Standard P802.3bs 200 Gb/s and 400 Gb/s. Available online: http://www.ieee802.org/3/bs/index.html (accessed on 6 December 2017).
26. Zhong, K.; Zhou, X.; Wang, Y.; Huo, J.; Zhang, H.; Zeng, L.; Yu, C.; Lau, A.P.T.; Lu, C. Amplifier-Less Transmission of 56Gbit/s PAM4 over 60km Using 25Gbps EML and APD. In Proceedings of the Optical Fiber Communications Conference (OFC), Los Angeles, CA, USA, 19–23 March 2017; p. Tu2D.1.
27. Nada, M.; Yoshimatsu, T.; Muramoto, Y.; Ohno, T.; Nakajima, F.; Matsuzaki, H. 106-Gbit/s PAM4 40-km transmission using an avalanche photodiode with 42-GHz bandwidth. In Proceedings of the Optical Fiber Communications Conference (OFC), San Diego, CA, USA, 11–15 March 2018; pp. 1–3.
28. Chan, T.K.; Way, W.I. 112 Gb/s PAM4 transmission over 40km SSMF using 1. In 3 μm gain-clamped semiconductor optical amplifier. In Proceedings of the Optical Fiber Communications Conference (OFC), Los Angeles, CA, USA, 22–26 March 2015; p. Th3A.4.
29. Stojanovic, N.; Karinou, F.; Qiang, Z.; Prodaniuc, C. Volterra and Wiener Equalizers for Short-Reach 100G PAM-4 Applications. *J. Lightw. Technol.* **2017**, *21*, 4583–4594. [CrossRef]
30. Li, X.; Zhou, S.; Ji, H.; Luo, M.; Yang, Q.; Yi, L.; Hu, Y.; Li, C.; Fu, S.; Alphones, A.; et al. Transmission of 4 × 28-Gb/s PAM-4 over 160-km single mode fiber using 10G-class DML and photodiode. In Proceedings of the Optical Fiber Communications Conference (OFC), Anaheim, CA, USA, 20–24 March 2016; pp. 1–3.
31. Gao, Y.; Cartledge, J.C.; Yam, S.S.H.; Rezania, A.; Matsui, Y. 112 Gb/s PAM-4 using a directly modulated laser with linear pre-compensation and nonlinear post-compensation. In Proceedings of the European Conference and Exhibition on Optical Communication (ECOC), Dusseldorf, Germany, 18–22 September 2016; pp. 1–3.
32. Zhang, Q.; Stojanovic, N.; Prodaniuc, C.; Karinou, F.; Xie, C. Cost-effective single-lane 112 Gb/s solution for 2 mobile fronthaul and access applications. *Opt. Express* **2016**, *24*, 5720–5723. [CrossRef]
33. Zhong, K.; Chen, W.; Sui, Q.; Man, J.W.; Lau, A.P.T.; Lu, C.; Zeng, L. Low cost 400 GE transceiver for 2 km optical interconnect using PAM4 and direct detection. In Proceedings of the Asia Communications and Photonics Conference (ACP), Shanghai, China, 11–14 November 2014; p. ATh4D.2.
34. Zhong, K.; Chen, W.; Sui, Q.; Man, J.W.; Lau, A.P.T.; Lu, C.; Zeng, L. Experimental demonstration of 500 Gbit/s short reach transmission employing PAM4 signal and direct detection with 25 Gbps device. In Proceedings of the Optical Fiber Communications Conference (OFC), Los Angeles, CA, USA, 22–26 March 2015; p. TH3A.3.
35. Zhong, K.; Zhou, X.; Gao, Y.; Chen, W.; Man, J.; Zeng, L.; Lau, A.P.T.; Lu, C. 140-Gb/s 20-km Transmission of PAM-4 Signal at 1.3 μm for Short Reach Communications. *Photon. Technol. Lett.* **2015**, *16*, 1757–1760. [CrossRef]
36. Zhang, K.; Zhuge, Q.; Xin, H.; Morsy-Osman, M.; El-Fiky, E.; Yi, L.; Hu, W.; Plant, D.V. Intensity-directed Equalizer for Chirp Compensation Enabling DML-based 56Gb/s PAM4 C-band Delivery over 35.9 km SSMF. In Proceedings of the European Conference and Exhibition on Optical Communication (ECOC), Gothenburg, Sweden, 17–21 September 2017.
37. Zhang, K.; Zhuge, Q.; Xin, H.; Morsy-Osman, M.; El-Fiky, E.; Yi, L.; Hu, W.; Plant, D.V. Intensity directed equalizer for the mitigation of DML chirp induced distortion in dispersion-unmanaged C-band PAM transmission. *Opt. Express* **2017**, *23*, 28123–28135. [CrossRef]
38. Zhou, H.; Li, Y.; Gao, C.; Li, W.; Hong, X.; Wu, J. Clock Recovery and Adaptive Equalization for 50 Gbit/s PAM4 Transmission. In Proceedings of the Asia Communications and Photonics Conference (ACP), Hangzhou, China, 26–29 October 2018.
39. Zhou, H.; Li, Y.; Lu, D.; Yue, L.; Gao, C.; Liu, Y.; Hao, R.; Zhao, Z.; Li, W.; Qiu, J.; et al. Joint clock recovery and feed-forward equalization for PAM4 transmission. *Opt. Express* **2019**, *8*, 11385–11395. [CrossRef] [PubMed]
40. Chen, G.; Du, J.; Sun, L.; Zhang, W.; Xu, K.; Chen, X.; Reed, G.T.; He, Z. Nonlinear Distortion Mitigation by Machine Learning of SVM Classification for PAM-4 andPAM-8 Modulated Optical Interconnection. *J. Lightw. Technol.* **2018**, *3*, 650–657. [CrossRef]

41. Miao, X.; Bi, M.; Yu, J.; Li, L.; Hu, W. SVM-Modified-FFE Enabled Chirp Management for 10G DML-based 50Gb/s/λ PAM4 IM-DD PON. In Proceedings of the Optical Fiber Communications Conference (OFC), San Diego, CA, USA, 3–7 March 2019; p. M2B.5.
42. Chen, G.; Du, J.; Sun, L.; Zheng, L.; Xu, K.; Tsang, H.K.; Chen, X.; Reed, G.T.; He, Z. Machine Learning Adaptive Receiver for PAM-4 Modulated Optical Interconnection Based on Silicon Microring Modulator. *J. Lightw. Technol.* **2018**, *18*, 4106–4113. [CrossRef]
43. Reza, A.G.; Rhee, J.K.K. Nonlinear Equalizer Based on Neural Networks for PAM-4 Signal Transmission Using DML. *Photonics Technol. Lett.* **2018**, *15*, 1416–1419. [CrossRef]
44. Yang, Z.; Gao, F.; Fu, S.; Li, X.; Deng, L.; He, Z.; Tang, M.; Liu, D. Radial basis function neural network enabled C-band 4 × 50 Gb/s PAM-4 transmission over 80 km SSMF. *Opt. Lett.* **2018**, *15*, 3542–3545. [CrossRef] [PubMed]
45. Li, P.; Yi, L.; Xue, L.; Hu, W. 56 Gbps IM/DD PON based on 10G-Class Optical Devices with 29 dB Loss Budget Enabled by Machine Learning. In Proceedings of the Optical Fiber Communications Conference (OFC), San Diego, CA, USA, 11–15 March 2018; pp. 1–3.
46. Chuang, C.; Liu, L.; Wei, C.; Liu, J.; Henrickson, L.; Huang, W.; Wang, C.; Chen, Y.; Chen, J. Convolutional Neural Network based Nonlinear Classifier for 112-Gbps High Speed Optical Link. In Proceedings of the Optical Fiber Communications Conference (OFC), San Diego, CA, USA, 11–15 March 2018; p. W2A.43.
47. Chuang, C.Y.; Wei, C.C.; Lin, T.C.; Chi, K.L.; Liu, L.C.; Shi, J.W.; Chen, Y.; Chen, J. Employing Deep Neural Network for High Speed 4-PAM Optical Interconnect. In Proceedings of the European Conference and Exhibition on Optical Communication (ECOC), Gothenburg, Sweden, 17–21 September 2017.
48. Luo, M.; Gao, F.; Li, X.; He, Z.; Fu, S. Transmission of 4 × 50-Gb/s PAM-4 Signal over 80-km Single Mode Fiber using Neural Network. In Proceedings of the Optical Fiber Communications Conference (OFC), San Diego, CA, USA, 11–15 March 2018; p. M2F.2.
49. Wan, Z.; Li, J.; Shu, L.; Luo, M.; Li, X.; Fu, S.; Xu, K. Nonlinear equalization based on pruned artificial neural networks for 112-Gb/s SSB-PAM4 transmission over 80-km SSMF. *Opt. Express* **2018**, *8*, 10631–10642. [CrossRef]
50. Li, P.; Yi, L.; Xue, L.; Hu, W. 100Gbps IM/DD Transmission over 25km SSMF using 20Gclass DML and PIN Enabled by Machine Learning. In Proceedings of the Optical Fiber Communications Conference (OFC), San Diego, CA, USA, 11–15 March 2018; p. W2A.46.
51. Yi, L.; Li, P.; Liao, T.; Hu, W. 100Gb/s/λ IM-DD PON using 20G-class optical devices by machine learning based equalization. In Proceedings of the European Conference and Exhibition on Optical Communication (ECOC), Rome, Italy, 23–27 September 2018.
52. Estaran, J.; Rios-Müller, R.; Mestre, M.A.; Jorge, F.; Mardoyan, H.; Konczykowska, A.; Dupuy, J.Y.; Bigo, S. Artificial Neural Networks for Linear and Non-Linear Impairment Mitigation in High-Baudrate IM/DD Systems. In Proceedings of the European Conference and Exhibition on Optical Communication (ECOC), Dusseldorf, Germany, 18–22 September 2016.
53. Houtsma, V.; Chou, E.; Veen, D. 92 and 50 Gbps TDM-PON using Neural Network Enabled Receiver Equalization Specialized for PON. In Proceedings of the Optical Fiber Communications Conference (OFC), San Diego, CA, USA, 3–7 March 2019; p. M2B.6.
54. Chang, F.; Bhoja, S. New Paradigm Shift to PAM4 Signalling at 100/400G for Cloud Data Centers: A Performance Review. In Proceedings of the European Conference and Exhibition on Optical Communication (ECOC), Gothenburg, Sweden, 17–21 September 2017.
55. Karinou, F.; Stojanovic, N.; Prodaniuc, C.; Qiang, Z.; Dippon, T. 112 Gb/s PAM-4 optical signal transmission over 100-m OM4 multimode fiber for high-capacity data-center interconnects. In Proceedings of the European Conference and Exhibition on Optical Communication (ECOC), Dusseldorf, Germany, 18–22 September 2016.
56. Matsui, Y.; Pham, T.; Ling, W.A.; Schatz, R.; Carey, G.; Daghighian, H.; Sudo, T.; Roxlo, C. 55-GHz Bandwidth Short-Cavity Distributed Reflector Laser and its Application to 112-Gb/s PAM-4. In Proceedings of the Optical Fiber Communications Conference (OFC), Anaheim, CA, USA, 20–22 March 2016; p. Th5B.4.
57. Kim, B.G.; Bae, S.H.; Kim, H.; Chung, Y.C. DSP-based CSO cancellation technique for RoF transmission system implemented by using directly modulated laser. *Opt. Express* **2017**, *11*, 12152–12160. [CrossRef]
58. Wei, C.; Cheng, H.; Huang, W. On adiabatic chirp and compensation for nonlinear distortion in DML-based OFDM transmission. *J. Lightw. Technol.* **2018**, *16*, 3502–3513. [CrossRef]

59. Zhang, K.; Zhuge, Q.; Xin, H.; Hu, W.; Plant, D.V. Performance comparison of DML, EML and MZM in dispersion-unmanaged short reach transmissions with digital signal processing. *Opt. Express* **2018**, *26*, 34288–34304. [CrossRef]
60. Zhang, Q.; Stojanovic, N.; Xie, C.; Prodaniuc, C.; Laskowski, P. Transmission of single lane 128 Gbit/s PAM-4 signals over an 80 km SSMF link, enabled by DDMZM aided dispersion pre-compensation. *Opt. Express* **2016**, *21*, 24580–24591. [CrossRef] [PubMed]
61. Kai, Y.; Nishihara, M.; Tanaka, T.; Takahara, T.; Li, L.; Tao, Z.; Liu, B.; Rasmussen, J.C.; Drenski, T. Experimental Comparison of Pulse Amplitude Modulation (PAM) and Discrete Multi-tone (DMT) for Short-Reach 400-Gbps Data Communication. In Proceedings of the European Conference and Exhibition on Optical Communication (ECOC), London, UK, 22–26 September 2013; pp. 1–3.
62. Filer, M.; Searcy, S.; Fu, Y.; Nagarajan, R.; Tibuleac, S. Demonstration and performance analysis of 4 Tb/s DWDM metro-DCI system with 100 G PAM4 QSFP28 modules. In Proceedings of the Optical Fiber Communications Conference (OFC), Los Angeles, CA, USA, 19–23 March 2017; pp. 1–3.
63. Zhang, J.; Wey, J.S.; Shi, J.; Yu, J.; Tu, Z.; Yang, B.; Yang, W.; Guo, Y.; Huang, X.; Ma, Z. Experimental Demonstration of Unequally Spaced PAM-4 Signal to Improve Receiver Sensitivity for 50-Gbps PON with Power-Dependent Noise Distribution. In Proceedings of the Optical Fiber Communications Conference (OFC), San Diego, CA, USA, 11–15 March 2018; pp. 1–3.
64. Castro, J.M.; Pimpinella, R.J.; Kose, B.; Huang, Y.; Novick, A.; Lane, B. Eye Skew Modeling, Measurements and Mitigation Methods for VCSEL PAM-4 Channels at Data Rates over 66 Gb/s. In Proceedings of the Optical Fiber Communications Conference (OFC), Los Angeles, CA, USA, 19–23 March 2017; p. W3G.3.
65. Rath, R.; Clausen, D.; Ohlendorf, S.; Pachnicke, S.; Rosenkranz, W. Tomlinson–Harashima Precoding for Dispersion Uncompensated PAM-4 Transmission with Direct-Detection. *J. Lightw. Technol.* **2017**, *18*, 3909–3917. [CrossRef]
66. Tang, X.; Liu, S.; Xu, X.; Qi, J.; Guo, M.; Zhou, J.; Qiao, Y. 50-Gb/s PAM4 over 50-km Single Mode Fiber Transmission Using Efficient Equalization Technique. In Proceedings of the Optical Fiber Communications Conference (OFC), San Diego, CA, USA, 3–7 March 2019; p. W2A.45.
67. Proakis, J.G.; Manolakis, D.G. *Digital Signal. Processing: Principles, Algorithms and Applications*, 4th ed.; Pearson Education: London, UK, 2007.
68. Haykin, S.S. *Adaptive Filter Theory*, 5th ed.; Pearson Education: Hamilton, ON, Canada, 2005.
69. Proakis, J.G. *Digital Communications*, 4th ed.; The McGraw-Hill Companies: San Diego, CA, USA, 2008.
70. Rath, R.; Rosenkranz, W. Tomlinson-Harashima Precoding for Fiber-Optic Communication Systems. In Proceedings of the European Conference and Exhibition on Optical Communication (ECOC), London, UK, 22–26 September 2013.
71. Matsumoto, K.; Yoshida, Y.; Maruta, A.; Kanno, A.; Yamamoto, N.; Kitayama, K. On the impact of Tomlinson-Harashima precoding in optical PAM transmissions for intra-DCN communication. In Proceedings of the Optical Fiber Communications Conference (OFC), Los Angeles, CA, USA, 19–23 March 2017; p. Th3D.7.
72. Kikuchi, N.; Hirai, R.; Fukui, T. Application of Tomlinson-Harashima Precoding (THP) for Short-Reach Band-Limited Nyquist PAM and Faster-Than-Nyquist PAM Signaling. In Proceedings of the Optical Fiber Communications Conference (OFC), San Diego, CA, USA, 11–15 March 2018; pp. 1–3.
73. Kikuchi, N.; Hirai, R.; Fukui, T.; Takashima, S. Modulator Non-Linearity Compensation in Tomlinson-Harashima Precoding (THP) for Short-Reach Nyquist- and Faster-than-Nyquist (FTN) IM/DD PAM Signaling. In Proceedings of the European Conference and Exhibition on Optical Communication (ECOC), Rome, Italy, 23–27 September 2018.
74. Zhou, X.; Chen, X.; Zhou, W.; Fan, Y.; Zhu, H.; Li, Z. All-Digital Timing Recovery and Adaptive Equalization for 112 Gbit/s POLMUX-NRZ-DQPSK Optical Coherent Receivers. *J. Opt. Commun. Netw.* **2010**, *11*, 984–990. [CrossRef]
75. Mathews, V.J. Adaptive polynomial filters. *IEEE Signal Process. Mag.* **1991**, *3*, 10–26. [CrossRef]
76. Zhu, A.; Pedro, J.C.; Cunha, T.R. Pruning the Volterra series for behavioral modeling of power amplifiers using physical knowledge. *Trans. Microw. Theory Tech.* **2007**, *5*, 813–821. [CrossRef]
77. Li, X.; Zhou, S.; Gao, F.; Luo, M.; Yang, Q.; Mo, Q.; Yu, Y.; Fu, S. 4 × 28 Gb/s PAM4 long-reach PON using low complexity nonlinear compensation. In Proceedings of the Optical Fiber Communications Conference (OFC), Los Angeles, CA, USA, 19–23 March 2017; p. M3H.4.

78. Lu, S.; Wei, C.; Chuang, C.; Chen, Y.; Chen, J. 81.7% Complexity Reduction of Volterra Nonlinear Equalizer by Adopting L1 Regularization Penalty in an OFDM Long-Reach PON. In Proceedings of the European Conference and Exhibition on Optical Communication (ECOC), Gothenburg, Sweden, 17–21 September 2017.
79. Huang, W.; Chang, W.; Wei, C.; Liu, J.; Chen, Y.; Chi, K.; Wang, C.; Shi, J.; Chen, J. 93% Complexity Reduction of Volterra Nonlinear Equalizer by L1-Regularization for 112-Gbps PAM-4 850-nm VCSEL Optical Interconnect. In Proceedings of the Optical Fiber Communications Conference (OFC), San Diego, CA, USA, 11–15 March 2018; pp. 1–3.
80. Ge, L.; Zhang, W.; Liang, C.; He, Z. Threshold based Pruned Retraining Volterra Equalization for PAM-4 100 Gbps VCSEL and MMF Based Optical Interconnects. In Proceedings of the Asia Communications and Photonics Conference (ACP), Hangzhou, China, 26–29 October 2018.
81. Samuel, A.L. Some Studies in Machine Learning Using the Game of Checkers. *J. Res. Dev.* **1959**, *3*, 210–229. [CrossRef]
82. Zibar, D.; Piels, M.; Jones, R.; Schäeffer, C.G. Machine learning techniques in optical communication. *J. Lightw. Technol.* **2016**, *6*, 1442–1452. [CrossRef]
83. Sebald, D.J.; Bucklew, J.A. Support vector machine techniques for nonlinear equalization. *IEEE Trans. Signal Process.* **2000**, *11*, 3217–3226. [CrossRef]
84. Chen, G.; Sun, L.; Xu, K.; Du, J.; He, Z. Machine learning of SVM classification utilizing complete binary tree structure for PAM-4/8 optical interconnection. In Proceedings of the Optical Interconnects Conference (OI), Santa Fe, NM, USA, 5–7 June 2017.
85. Ito, K.; Niwa, M.; Ueda, K.; Mori, Y.; Hasegawa, H.; Sato, K.I. Impairment mitigation in non-coherent optical transmission enabled with machine learning for intra-datacenter networks. In Proceedings of the Next-Generation Optical Networks for Data Centers and Short-Reach Links, San Francisco, CA, USA, 28 January 2017.
86. Lyubomirsky, I. Machine learning equalization techniques for high speed PAM4 fiber optic communication systems. In *CS229 Final Project Report*; Stanford University: Stanford, CA, USA, 2015.
87. Zeng, Z.; Yu, H.; Xu, H.; Xie, Y.; Gao, J. Fast training support vector machines using parallel sequential minimal optimization. In Proceedings of the International Conference on Intelligent System and Knowledge Engineering, Xiamen, China, 17–19 November 2008; pp. 997–1001.
88. Specht, D.F. A general regression neural network. *Trans. Neural Netw.* **1991**, *6*, 568–576. [CrossRef]
89. Eriksson, T.A.; Bülow, H.; Leven, A. Applying Neural Networks in Optical Communication Systems: Possible Pitfalls. *Photonics Technol. Lett.* **2017**, *23*, 2091–2094. [CrossRef]
90. Wang, D.; Zhang, M.; Li, J.; Li, Z.; Li, J.; Song, C.; Chen, X. Intelligent constellation diagram analyzer using convolutional neural network-based deep learning. *Opt. Express* **2017**, *15*, 17150–17166. [CrossRef] [PubMed]
91. Khan, F.N.; Zhou, Y.; Lau, A.P.T.; Lu, C. Modulation format identification in heterogeneous fiber-optic networks using artificial neural networks. *Opt. Express* **2012**, *11*, 12422–12431. [CrossRef] [PubMed]
92. Zhou, S.; Li, X.; Yi, L.; Yang, Q.; Fu, S. Transmission of 2 × 56 Gb/s PAM-4 signal over 100 km SSMF using 18 GHz DMLs. *Opt. Lett.* **2016**, *8*, 1805–1808. [CrossRef] [PubMed]
93. Gao, F.; Zhou, S.; Li, X.; Fu, S.; Deng, L.; Tang, M.; Liu, D.; Yang, Q. 2 × 64 Gb/s PAM-4 transmission over 70 km SSMF using O-band 18G-class directly modulated lasers (DMLs). *Opt. Express* **2017**, *7*, 7230–7237. [CrossRef] [PubMed]